PHYSICA B

Recognized by the European Physical Society

CONDENSED MATTER

Proceedings of the Seventh
International Conference on Electrical
Transport and Optical Properties of
Inhomogeneous Media

ETOPIM-7

held in Sydney, Australia
9–13 July 2006

Guest Editors:
Ross C. McPhedran
Nicolae-Alexandru P. Nicorovici
Boris T. Kuhlmey
Lindsay C. Botten

Available online at
ScienceDirect
www.sciencedirect.com

http://www.elsevier.com/locate/physb

ELSEVIER

Near-field, broadband optical spectroscopy of metamaterials

Reuben M. Bakker*, Vladimir P. Drachev, Hsiao-Kuan Yuan, Vladimir M. Shalaev

Electrical and Computer Engineering and the Birck Nanotechnology Center, Purdue University, West Lafayette, IN, USA

Abstract

Near-field, broadband optical spectroscopy of metamaterials is reported. A compact, easy to assemble supercontinuum light source, coupled with a near-field scanning optical microscope and spectrometer provide the means to locally probe the spectral response of a nanorod metamaterial sample. Spectral maps of near-field transmittance are obtained for the spectral range from 500 to 950 nm. In comparison to far-field measurement, the average of the near-field mappings shows a significant increase in transmittance. The uniqueness of the spectral maps and the increased transmittance indicates a strong nanoantenna effect between the sample and the plasmonic near-field aperture.

1. Introduction

Near-field scanning optical microscopy enables one to probe light–matter interactions on a scale not possible with conventional optical microscopy. This type of scanning probe microscopy has been developed over the past 20 years and became commercially viable approximately a decade ago. Basic principles of the technique are well discussed in several review articles [1,2].

Typically, a near-field scanning optical microscope (NSOM) uses single-wavelength sources to probe local optical responses. Replacing a narrowband light source with a broadband source allows one to study the sample of interest with a wide range of wavelengths simultaneously. The first recorded use of this technique applied an incoherent white light lamp source to an apertureless NSOM configuration [3]. Later, this approach was extended to an aperture-based NSOM with an incoherent light source [4]. This is the first and only example currently found in the literature showing two-dimensional white light spectral mappings broken down into a series of mappings for different wavelength ranges. A white light NSOM with a coherent source was first demonstrated where the broadband spectrum was generated in a sapphire plate pumped by a femtosecond Ti:sapphire laser [5]. A further variant on this scheme uses a photonic crystal fibre as the nonlinear element to generate white light [6].

Expanding on the idea of adding a spectral component to near-field microscopy, we have put together a self-sufficient broadband light source based on pumping 20 m of photonic crystal fibre with a 1064 nm pulsed laser. Utilizing a broadband source with high-spatial coherence as the illumination light for a NSOM and a spectrometer allows for the ability to obtain NSOM images within a broad spectral range in a single experiment. Such instrumentation can be extremely useful in studies of novel plasmonic materials such as percolation thin films, nanoantennae, nanowires, voids in metallic films and general nano- and meso-ordered and disordered samples.

In this paper, we study local spectroscopy of metamaterials engineered as potential materials with optical magnetism and negative refractive index. By definition, metamaterials have features smaller than the wavelength of light. Optical spectroscopy in the near field will provide an additional dimension for metamaterial characterization.

*Corresponding author.

E-mail address: rbakker@purdue.edu (R.M. Bakker).

The instrumentation and subsequent imaging results in this paper present a first application of local broadband spectroscopy to metamaterials.

2. Experimental setup

This version of broadband, near-field spectroscopy consists of mating three tools: a home-built supercontinuum light source; a commercially obtained near-field scanning optical microscope (Nanonics Imaging, Israel [7]); and a spectrometer (Renishaw, United Kingdom [8]). A general schematic of the equipment is shown in Fig. 1a. The supercontinuum source is based upon pumping a geometrically tailored photonic crystal fibre (Crystal Fibre, Denmark [9]) with a pulsed microchip laser operating at 1064 nm (JDS Uniphase, USA [10]). The output of the supercontinuum is used as the light source for the illumination mode NSOM. A cantilevered, aperture-based NSOM probe, drawn from a length of single-mode fibre delivers light to the sample. The probe has a gold coating on the fibre surface with the aperture of about 150 nm in diameter. The tapering and bending of the fibre leads to a linear polarization of the light at the NSOM probe output. The polarization was measured to be at least 80% linear.

Using a piezoelectric scanning platform, the fibre probe and the sample are brought together within a controlled distance using atomic force microscopy (AFM) feedback based on a tuning fork response. The sample is raster scanned with the probe held stationary in its lateral position. Transmitted light is collected using a 100X, 0.75 NA objective lens externally coupled to a spectro-

meter. The spectrometer contains a monochromator and a thermoelectrically cooled charge-coupled device (CCD). Typical NSOM imaging with an avalanche photodiode for light detection requires a stationary time of approximately 10 ms for each pixel. The spectrometer used for this experiment requires several grating positions to cover needed spectral range, it takes approximately 2 min per each pixel to obtain the desired spectrum. Thus, spectra are taken at selected pixels only.

All local transmission spectra for a sample need to be normalized per a set of reference spectra (through bare substrate) that are obtained before and after the data collection on the sample. The average reference spectrum used for the presented experimental results is shown in Fig. 1b. By comparing the data from each spectral acquisition, the percent transmission for each pixel can be found. Data for one and two dimensional, spectral and spatial mappings, can be created.

As collecting sufficient spectral data to create a two-dimensional spectral mapping can take up to and beyond 1 day, the long-term stability of the instrumentation has been evaluated. Preliminary measurements show spatially localized and wavelength-specific variances of up to 30% when a spectral map is created over a bare glass substrate. On average, over time and wavelength such variances are typically much lower than 30%.

3. Imaging of metamaterials

As a first application of this unique instrumentation, we study an array of double layered gold nanorods. This sample was studied recently in far-field experiments to demonstrate a negative refractive index material at 1.5 μm [11,12]. Details of sample geometry and a representative field emission scanning electron microscope (SEM) image are shown in Fig. 2.
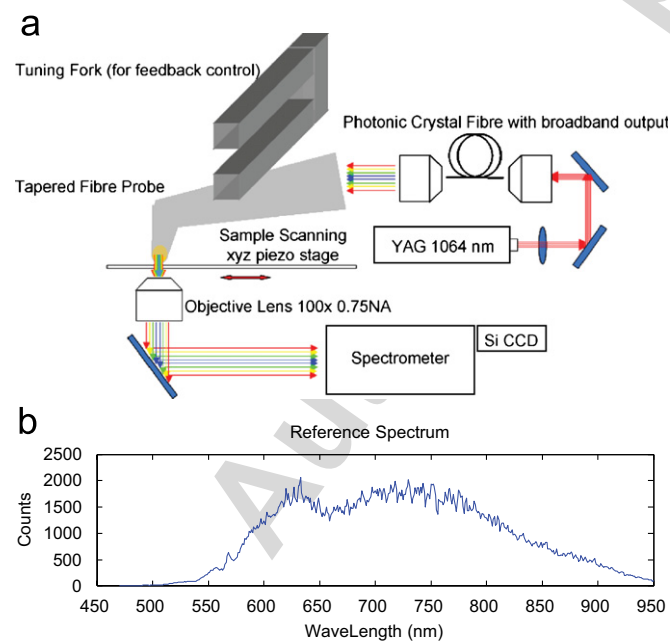

Fig. 1. Experimental conditions: (a) experimental set-up, consisting of a supercontinuum light source based on pumping a photonic crystal fibre, an AFM/NSOM based on a tuning fork and aperture tip and a spectrometer with a Si CCD. (b) The reference spectrum of the system, in transmission mode, with only bare glass as the sample.
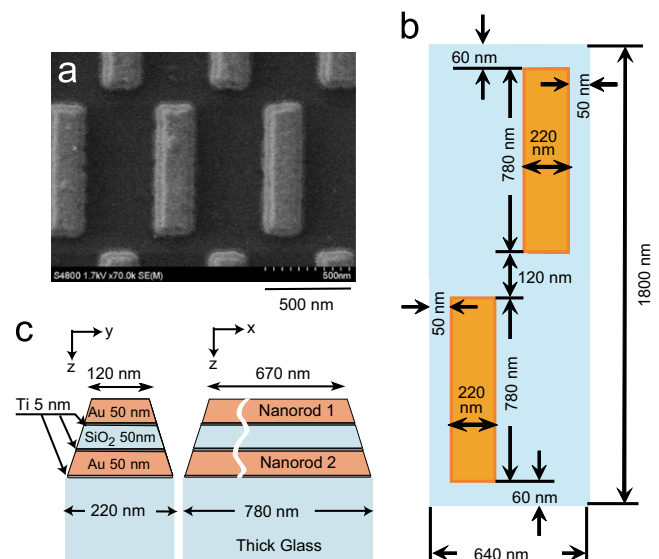

Fig. 2. The nanorod sample: (a) characteristic SEM image, (b) unit cell geometry and (c) Z profile.

Data was collected during a $2.5 \times 2.5\,\mu m$ scan using 256 pixels per side for the AFM image. The orientation of the sample in reference to the NSOM aperture dictated that the illuminating near-field light was polarized across the rods, which is termed perpendicular polarization. Broadband spectroscopy data were collected every seven pixels in a 36×29 array, giving a spacing of approximately 68 nm between each of the collected spectra. A set of reference spectra were collected with the aperture over the bare substrate before and after the mapping dataset. These were used to define transmittance as

$$T(x, y, \lambda) = I(x, y, \lambda)/I_0(\lambda),$$

where $I(x,y,\lambda)$ is the spectrum intensity at a specific wavelength measured at the spatial coordinates (x,y) and $I_0(\lambda)$ is the average reference spectral intensity.

Two-dimensional spectral imaging maps of a unit cell were produced. Each spectral imaging map was obtained by averaging the maps from three unit cells. A spectral range of 26 nm produced 18 mappings from 500 to 950 nm. Five representative spectral ranges are shown in Fig. 3(a–e). The corresponding AFM image, showing the three unit cells, is seen in Fig. 3(f).

The AFM image collected along with the time spectral mapping shows obvious and systematic distortion of the nanorod array as compared with both SEM and typical AFM imaging. This is due to piezoelectric drift in the scanning stage during the approximately 35 h of collection time. Due to the fact that the distortion is systematic it can safely be ignored for the purposes of data interpretation. Additionally, the interaction area of the NSOM aperture (AFM tip) with the sample was measured on a portion of the sample possessing a distinct break in periodicity. Thus, the positions of the rods are known and can be correlated with the broadband NSOM mappings.

Upon examination of the mappings, a clear spectral dependence of the local transmittance is observed. In the 500 nm range, the transmittance is strongest, with values over 100% seen around the rods and 60% through the rods. Transmittance decreases as the wavelength is increased. Unexpectedly, the mapping of local transmittance contorts itself through the available wavelength range. This is especially evident in the 700 nm to low 800 nm range, where the spectral maps show little resemblance to the actual nanorod structure. At the high end of our spectral capabilities, the lowest transmittance is seen and the mappings begin to correspond to the structural geometry.

Alternatively and more quantitatively, the overall average near-field transmittance as a function of wavelength was examined. The near-field large area average transmittance obtained from the experiment described above is compared with far-field experimental data in Fig. 4. The trends of both experimental transmittance data sets are very close, but it is clearly seen that the near-field average shows 20–30% higher transmittance than the far-field result.
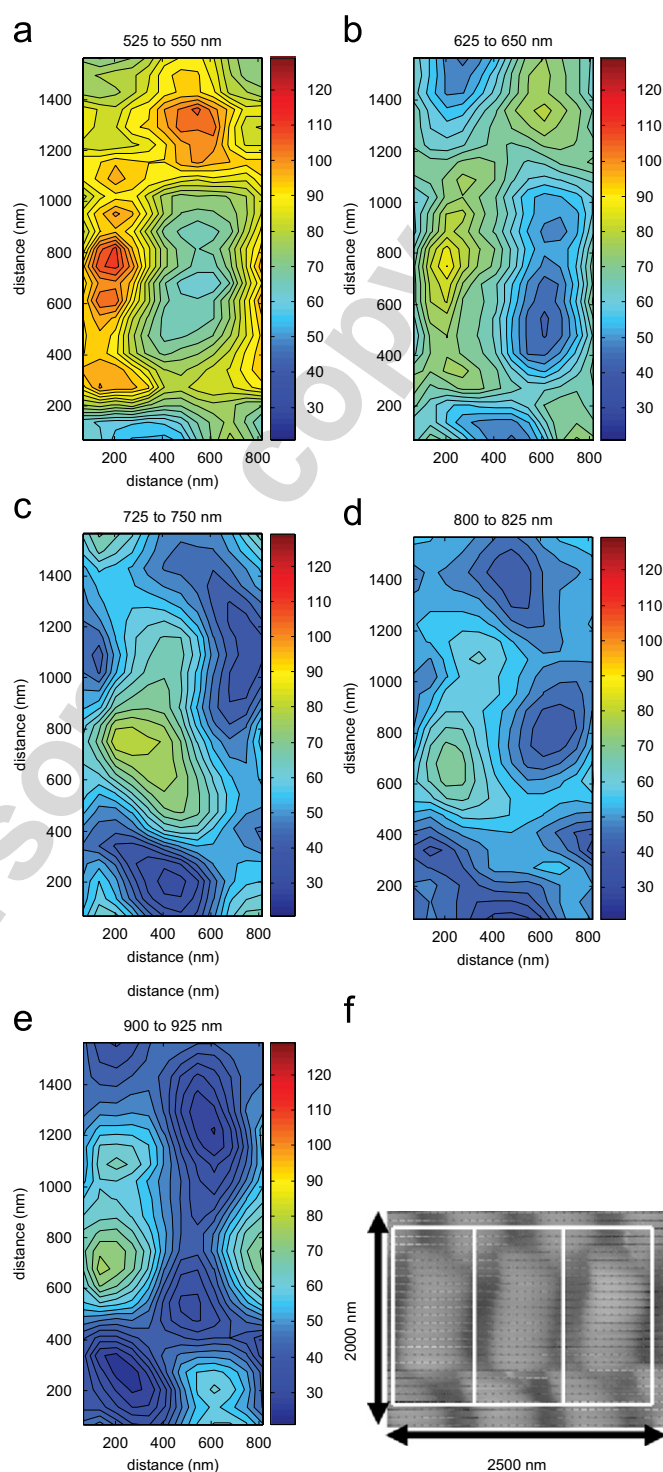

Fig. 3. Near-field spectral mapping, transmittance (from 20% to 130%): (a) 525–550 nm, (b) 625–650 nm, (c) 725–750 nm, (d) 800–825 nm (e) 900–925 nm and (f) the corresponding AFM image from the data collection, showing data collection points and the three 'unit cells' that were averaged.

Higher near-field average transmittance along with the strong spectral dependence of the wavelength mappings strongly suggest a nanoantenna effect between the gold coated tip and the individual sample structures. Structure–tip interaction effects are characterized by rich local
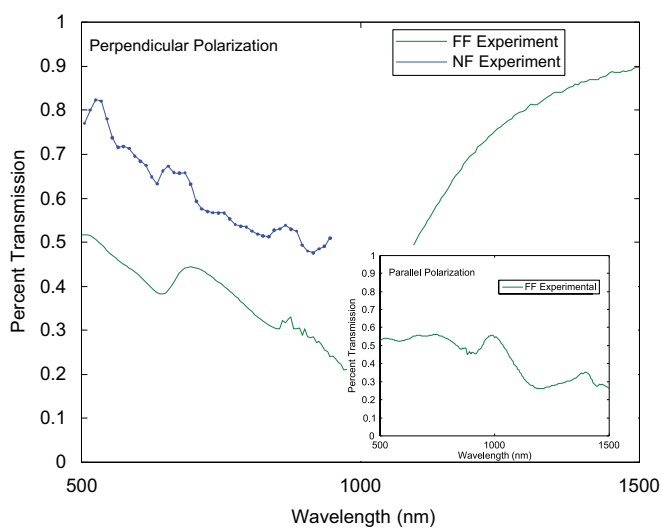
Fig. 4. Large area average transmission: the near-field broadband transmittance is averaged for all data points and compared with far-field transmittance data taken with a white lamp spectrometer for light polarized perpendicular to the rods. Inset is the far-field experimental result for parallel polarized light.

spectra, strong spectral dependence in the mappings, complex modes and higher than expected transmittance, all of which are seen in the experimental results presented. An example illustrating such a nanoantenna effect between a plasmonic sample and a plasmonic tip has been recently reported [13]. Here, strong spectral dependence in both the intensity and its spatial distribution due to the tip–nanostructure interaction are easily observed.

4. Conclusions

Broadband spectroscopy has been added to near-field scanning optical microscopy using a simple, self-sufficient supercontinuum generation scheme. While this is not the first implementation of broadband spectroscopy with near-field optics, this specific technique appears to be unique and easy to use in comparison with other methods.

Spectral mappings of a double-layer gold nanorod sample were obtained for the first time. Analysis of the near-field transmittance shows rich local spectral mappings along with enhanced average transmittance of 20–30% when compared with far-field techniques. This suggests a strong nano-antenna effect between the sample and the gold coated NSOM aperture.

Simple implementation of this technique applied to aperture near-field microscopy should be encouraging to the near-field optics community. Broadband spectroscopy adds a new dimension to near-field microscopy that has not yet seen sustained experimental efforts. Local broadband spectroscopy is a powerful experimental technique that will allow intimate spectral mapping of meso- and nano- sized structures. This method will allow experimentalists to determine wavelengths of the plasmon resonances.

Full exploitation of this instrumentation is an ongoing effort. The results presented are merely the beginning of a push towards a detailed understanding of the local, spectral response of a variety of metamaterials.

References

[1] R.C. Dunn, Chem. Rev. 99 (1999) 2891.
[2] B. Hecht, B. Sick, U.P. Wild, V. Deckert, R. Zenobi, O.J.F. Martin, D.W. Pohl, J. Chem. Phys. 112 (2000) 7761.
[3] L. Aigouy, F.X. Andreani, A.C. Boccara, J.C. Rivoal, J.A. Porto, R. Carminati, J.-J. Greffet, R. Megy, Appl. Phys. Lett. 76 (2000) 397.
[4] J. Seidel, S. Grafstrom, Ch. Loppacher, S. Trogisch, F. Schlaphof, L.M. Eng, Appl. Phys. Lett. 79 (2001) 2291.
[5] A.A. Mikhailovsky, M.A. Petruska, M.I. Stockman, V.I. Klimov, Opt. Lett. 18 (2003) 1686.
[6] T. Nagahara, K. Imura, H. Okamoto, Rev. Sci. Instrum. 75 (2004) 4528.
[7] Nanonics Imaging Ltd. Israel, ⟨www.nanonics.co.il⟩
[8] Renishaw plc United Kingdom, ⟨www.renishaw.com⟩
[9] Crystal Fibre A/S Denmark, ⟨www.crystal-fibre.com⟩
[10] JDS Uniphase Corporation United States of America, ⟨www.jdsu.com⟩
[11] V.M. Shalaev, W. Cai, U.K. Chettiar, H.-K. Yuan, A.K. Sarychev, V.P. Drachev, A.V. Kildishev, Opt. Lett. 30 (2005) 3356.
[12] V.P. Drachev, W. Cai, U. Chettiar, H.-K. Yuan, A.K. Sarychev, A.V. Kildishev, G. Klimeck, V.M. Shalaev, Laser Phys. Lett. 3 (2006) 49.
[13] V.P. Drachev, V.M. Shalaev, A.K. Sarychev, Raman imaging and sensing apparatus employing nanoantennas, US Patent No. 6 985 223 B2, 2006.